Effects of Horizontal Tail Ice on Longitudinal Aerodynamic Derivatives

R. J. Ranaudo*
NASA Lewis Research Center, Cleveland, Ohio 44135
J. G. Batterson†
NASA Langley Research Center, Hampton, Virginia 23665
A. L. Reehorst§ and T. H. Bond§
NASA Lewis Research Center, Cleveland, Ohio 44135
and
T. M. O'Mara¶
George Washington University, Washington, D.C. 20052

Flight tests were performed with the NASA Lewis Research Center's DH-6 icing research aircraft to determine the accuracy with which the effects of ice on aircraft longitudinal stability and control could be measured. Flights were made with both a clean (baseline) configuration and with simulated ice on the horizontal tail. At a given trim speed 45 repeat doublet maneuvers were performed in each of four test configurations to determine the ensemble variation of the estimated stability and control derivatives. Additional maneuvers were also performed in each configuration to determine the variation in the longitudinal derivative estimates over a wide range of trim speeds. Stability and control derivatives were estimated by a modified stepwise regression (MSR) technique. A measure of the confidence in the derivative estimates was obtained by comparing the standard error for the ensemble of repeat maneuvers to the average of the estimated standard errors predicted by the MSR program. The magnitude of icing effects on the derivative estimates was strongly dependent on flight speed and aircraft wing flap configuration. With wing flaps up, the estimated derivatives were degraded most at lower speeds corresponding to that configuration. With wing flaps extended to 10 deg, the estimated derivatives were degraded most at the higher corresponding speeds.

Nomenclature

b	= wing span, m
C_l, C_m, C_n	= roll, pitch, and yaw moment coefficients, respectively
C_X, C_Y, C_Z	= longitudinal, lateral, and vertical force coefficients, respectively
$\bar{c}$	= mean aerodynamic chord, m
c.g.	= aircraft center of gravity
g	= acceleration due to gravity
I_X, I_Y, I_Z	= moments of inertia, kg-m^2
I_{XZ}	= product of inertia, kg-m^2
J_{sr}	= cost function for stepwise regression algorithm
m	= aircraft mass, kg
N,n	= number of points
p,q,r	= roll, pitch, and yaw rates, respectively, rad/s or deg/s
S	= wing area, m^2
u,v,w	= longitudinal, lateral, and vertical velocity components, respectively
V	= total airspeed, $= (u^2+v^2+w^2)^{1/2}$, m/s or kt
$x_j(i)$	= measured aircraft response or control surface input
α	= corrected (freestream) angle of attack, rad or deg
β	= angle of sideslip, rad or deg
δe	= elevator deflection, rad or deg
θ,ϕ	= pitch and roll angles, respectively, rad or deg
ρ	= air density, kg/m^3

Presented as Paper 89-0754 at the AIAA 28th Aerospace Sciences Meeting, Reno, NV, Jan. 8-11, 1989; received July 24, 1989; revision received April 6, 1990; accepted for publication June 20, 1990.

*Senior Research Pilot. Member AIAA.
†Assistant Branch Head, Spacecraft Controls.
§Aerospace Engineer. Member AIAA.
¶Graduate Research Scholar.

Introduction

MODERN transport aircraft, certified for flight in icing conditions, normally employ ice protection systems to prevent ice from accumulating on critical lifting components. If these systems fail, or are improperly operated, ice can form on these components and pose a serious threat to safe flight characteristics. This problem, which is a continual concern for current generation aircraft, will be of even greater concern for future generation aircraft employing advanced propulsion systems and optimized aerodynamic designs. For example, high-propulsive efficiency engines such as propfans may not provide sufficient bleed air for wing and tail anti-icing. The use of energy-efficient deicing systems, which require some small buildup of ice before activation, will be their likely replacement. Aircraft equipped with these systems will have to demonstrate acceptable flying qualities with some leading-edge ice contamination, especially when flown in the takeoff or landing configuration. This requirement also applies to aircraft whose aerodynamic efficiency, enhanced by advanced airfoil designs and relaxed static stability criterion, is degraded when small leading-edge ice formations occur between deicing cycles. Likewise, aircraft employing full flight control augmentation must also display an acceptable tolerance to these small ice accretions and to those larger accretions caused by ice protection system failures or operator errors.

Currently, no analysis methodologies exist that provide the capability to predict the effect of icing on aircraft flight characteristics. Therefore, within the scope of the NASA Lewis Research Center's aircraft icing research program, a high priority has been assigned in measuring the effects of icing on aircraft performance and stability and control. Experimental data acquired from flight tests provide the basis for validating icing effects methodologies and for establishing correlations between computational codes, wind tunnel tests, and full-scale flight tests. Performance testing, which was extensively discussed in Refs. 1 and 2, provided reasonably consistent results and a high degree of confidence in measurement accuracy. As a result, these data are now being used in validating current methodologies that predict ice shape growth and their effect on aerodynamic performance. However, initial flight testing to estimate effects of icing on aircraft stability and control derivatives showed that the results could be obscured by the inherent problem of not knowing the true accuracy of the derivative estimates. Stability and control flight testing as reported in Refs. 3 and 4 used an early version of modified maximum likelihood estimation (MMLE) technique to estimate the derivative values. The accuracies of these derivative estimates were obtained by an approximation to the Cramer-Rao bound given by the maximum likelihood algorithm. Because it was known that these error estimates

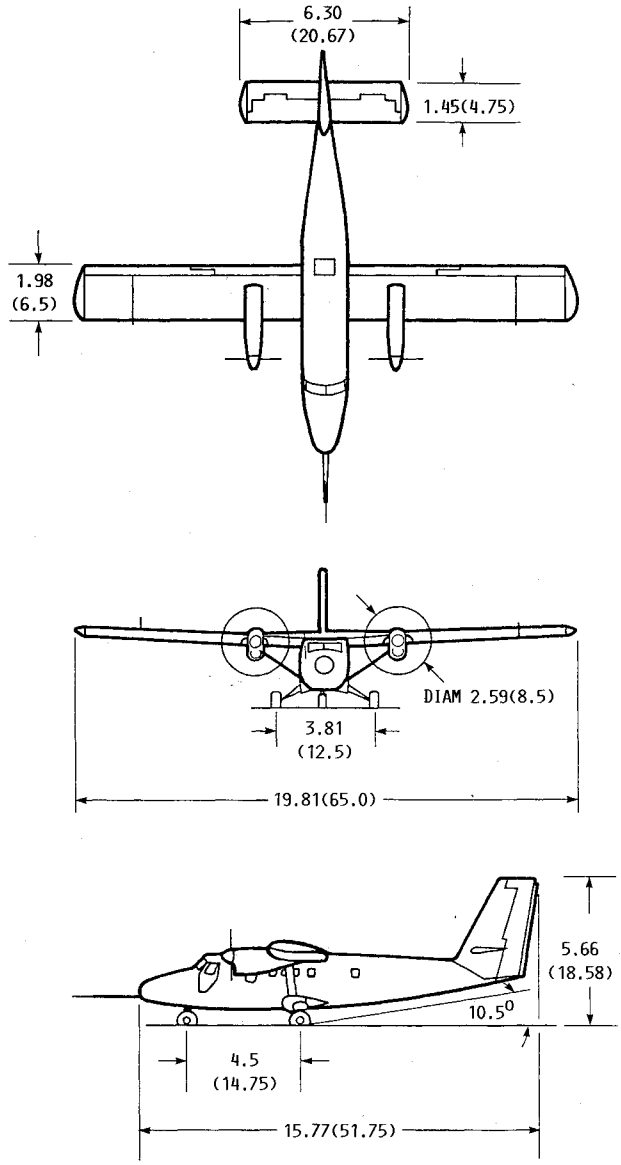

Fig. 1 NASA Lewis Research Center icing research aircraft: all dimensions are in meters (ft).

Table 1 Physical characteristics of the Dehavilland DH-6 Twin Otter

Characteristic	Low	High
Geometric:		
Wing area, m^2	39.02	
Wing span, m	19.81	
Aspect ratio	10	
MAC, m	1.981	
Mass, kg	4150	4600
Inertias, kg m^2:		
I_{xx}	21,279	21,787
I_{yy}	30,000	31,027
I_{zz}	44,986	48,639
I_{xz}	1432	1498

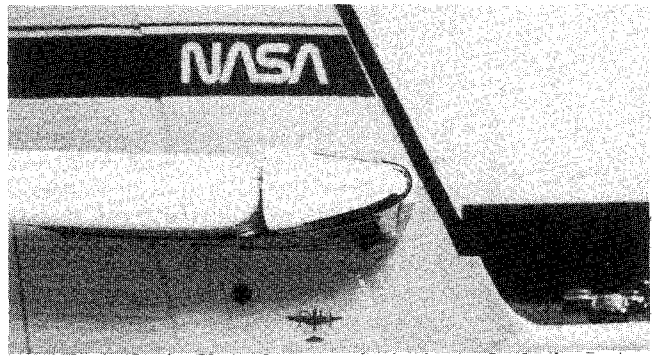

Fig. 2 Artificial moderate glaze ice attached to the tail of the icing research aircraft.

indicated higher accuracies than those that can be achieved by repeated experiments,[5] and because the differences between derivatives from the baseline and iced aircraft were found to be small, it was decided to conduct further flight testing to determine a realistic accuracy with which stability and control derivatives could be estimated. The purpose of this paper is to report on the results of those tests and to present the conclusions drawn from the data analysis programs.

For simplicity, the flight test plan was structured to examine only the longitudinal short-period characteristics of the research aircraft. Four data collection flights were defined: two flights were flown clean and two flights were flown with an artificial ice shape (described later in this report) attached to the leading edge of the horizontal tail.

Additional small amplitude doublets were then performed in each configuration at incrementally higher angles of attack (lower trim speeds). Power settings associated with each flap configuration remained constant for these maneuvers; therefore, doublet maneuvers initiated at the lower trim speeds were performed in climbs through a median test altitude.

Flight test maneuvers consisted of numerous repeat elevator doublets at a specified trim condition to determine the ensemble standard deviation for the parameter estimates. Additional maneuvers were also flown over the entire level flight angle-of-attack envelope to obtain derivative estimates for different flight conditions. Flight test maneuvers were analyzed using a modified stepwise regression (MSR) algorithm. The results are discussed relative to the accuracy of the derivative estimates and to the differences between the estimates obtained for the uniced vs iced horizontal tail. Some conclusions are also drawn as to the physical interpretation of the derivative estimates and their relevance to aircraft handling characteristics. Following the Introduction, this paper is organized in sections that describe the research airplane, instrumentation, flight test maneuvers, data reduction and analysis techniques, accuracy of the derivative estimates, effects of tail ice on handling characteristics, and conclusions.

Research Aircraft

The NASA Lewis icing research aircraft, shown in Fig. 1, is a modified DeHavilland DH-6 Twin Otter. It is powered by two 550-shp Pratt and Whitney PT6A-20A turbine engines driving three-bladed Hartzell constant-speed propellers. Physical dimensions, mass, and inertia specifications for the aircraft are found in Table 1.

For flights where an artificial ice shape was used to simulate a moderate glaze icing condition on the tail, formed aluminum caps were placed over the left and right leading edges of the horizontal tail and held in place with straps and clamps. Artificial ice cut from styrofoam was then secured to the tail caps with double-sided tape. The geometry and positioning of the artificial ice was based on an actual tail icing condition recorded on an earlier research flight in natural icing clouds. The entire arrangement is shown in Fig. 2.

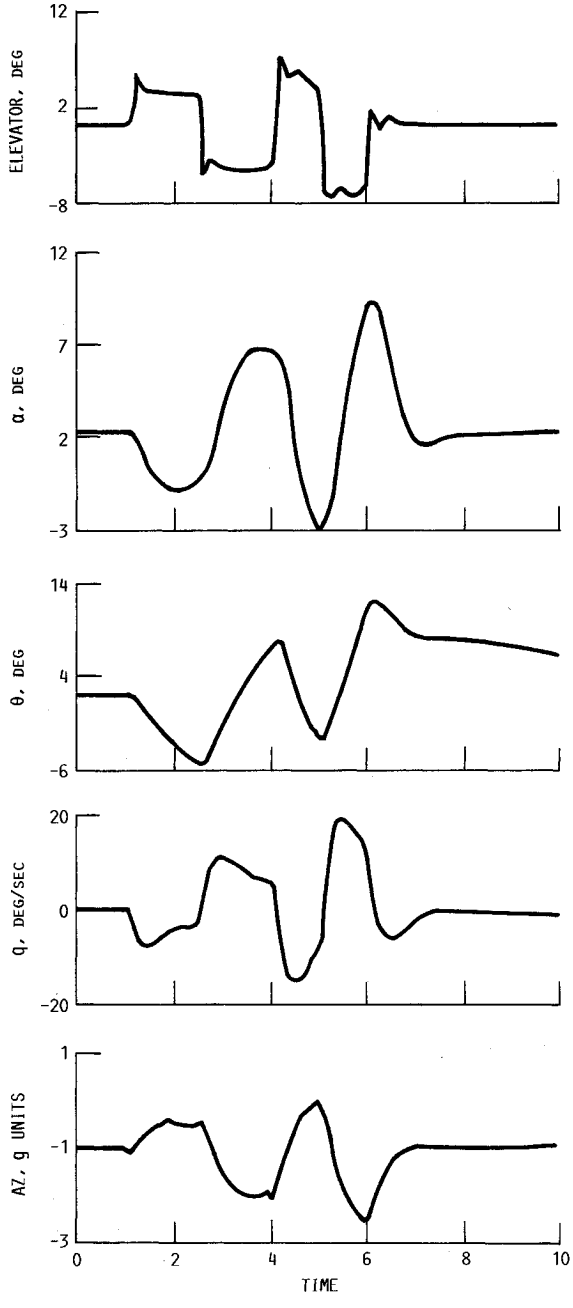

Fig. 3 Control surface input and aircraft response for a typical "2–1" elevator doublet.

Instrumentation

The icing research aircraft was equipped with three linear control position transducers (CPT) to measure the position of the elevator, ailerons, and rudder. The elevator CPT measured elevator position at the control horn to eliminate corrections for cable stretch. Flap position, constant for a given maneuver, was manually recorded from the flap position indicator in the cockpit.

Airspeed, pressure altitude, angle of attack, and angle of sideslip were measured by means of of sensors located on the flight test nose boom. Pitot-static pressures were sensed by a Rosemount 858 probe, which had been calibrated by the trailing-cone method. The high-frequency response angle-of-attack and angle-of-sideslip vanes were constructed from balsa wood and balanced by a heavy-metal counterweight. Angle of attack was referenced to the fuselage reference line, which is coincident with the aircraft floor line, and angle of sideslip was referenced to the aircraft longitudinal axis.

Kohlman Systems Research (KSR), Inc., Lawrence, Kansas, under contract to NASA, provided a stability and control data acquisition system (DAS). This system consisted of an attitude gyro, three axis orthogonal accelerometers, three axis angular rate gyros, and a digital data recording system that recorded 21 channels of flight test parameters with 12 bits per channel. All data were recorded on board at 20 samples per second (SPS), and all channels were sampled within one millisecond by the DAS.

Flight Testing

The center of gravity of the aircraft was measured experimentally. These measurements represented the zero-fuel weight characteristics of the aircraft and were corrected in the analysis program for actual crew and fuel weights recorded during each flight test maneuver.

Longitudinal stability and control flight testing was accomplished in four airplane configurations defined according to wing-flap setting and the simulated icing condition of the horizontal tail plane. The configurations were 1) clean tail, wing flaps up (0 deg); 2) clean tail, wing flaps 10 deg; 3) artificial horizontal tail icing, wing flaps up (0 deg); and 4) artificial horizontal tail icing, wing flaps 10 deg.

A constant engine power setting associated with each wing-flap condition was used while executing flight test maneuvers. This eliminated engine power as a variable in the derivative estimates. For the 0-deg wing-flap cases, 275 shp/engine was used and 219 shp/engine was used in the 10-deg wing-flap cases.

The standard small amplitude input was a "2–1" elevator doublet, which was designed to excite the short-period longitudinal mode of the airplane. A typical example of one of these doublet maneuvers is shown in Fig. 3.

Forty-five sets of identical small amplitude doublets were performed at a given flight condition in each configuration to determine the accuracy of the longitudinal stability and control derivative estimates. For the 0-deg flap configurations, repeat doublets were initiated from a level, unaccelerated flight condition at a trim speed of 120 kt indicated airspeed (KIAS). For the 10-deg flap configurations, these doublets were initiated from a level, unaccelerated flight condition at a trim speed of 100 KIAS.

Data Reduction and Analysis Technique

The recorded cassette tapes from each flight were initially sent to KSR, Inc., where the data were reduced to engineering units and rewritten on nine-track magnetic tape. These data sets were then transferred to the NASA Langley Research Center, Aircraft Guidance and Control Branch, for stability and control analysis.

The first step in the analysis procedure was to correct the measured data for all known errors. All sensor data were corrected for c.g. offset, angle-of-attack data were corrected

for upwash and boom bending effects, and several flight maneuvers were analyzed with a maximum likelihood algorithm[6] to estimate instrument biases and scale factors. These estimated corrections, when applied to the measured data, produced data sets that were ready for model structure determination and parameter estimation.

For the model structure determination procedure, it was assumed that

1) The general equations of rigid-body motion adequately define the airplane motion (see the Appendix).

2) The model for the aerodynamic force and moment coefficients can be represented by multivariable polynomials in response and control variables. The parameters in these equations are the coefficients of the Taylor series expansion around the values corresponding to the initial steady-state flight.

3) Linear terms in the Taylor series expansion make generally larger contribution to aerodynamic functions, followed by higher-order terms.

The third assumption, resulting in a constraint on the selection of significant terms in the regression equation, is what gives rise to the MSR technique.

MSR is a modified version of linear regression, which can determine the structure of the aerodynamic model equations and estimate the model parameters. The determination of an adequate model for the aerodynamic coefficients includes three steps: the postulation of terms that might enter the model, selection of an adequate model, and the verification of the model selected. The general form of aerodynamic model equations can be written as

$$y(t) = \theta_0 + \theta_1 x_1(t) + \cdots + \theta_n x_n(t) \qquad (1)$$

where $y(t)$ represents the resultant coefficient of aerodynamic force or moment. In the polynomial representation of the aerodynamic coefficient, θ_1 to θ_n are the stability and control derivatives, θ_0 is the value of any particular coefficient corresponding to the initial steady-flight conditions, and x_1 to x_n are the regressors formed by the increments in airplane output

Table 2 Mean values of stability and control derivatives calculated from 45 repeat maneuvers using modified step regression (0-deg flaps, 120 KIAS, baseline—no ice)

Parameter	Mean value, $\bar{\theta}$	Standard errors $s_E(\theta)$[a]	Standard errors $s(\theta)$[b]	Ratio, $s_E(\theta)/s(\theta)$
CZ_α	−5.66	0.0493	0.0169	2.9
Cz_q	−19.97	1.047	0.386	2.7
$Cz_{\delta e}$	−0.608	0.0281	0.0122	2.3
$C_{m\alpha}$	−1.31	0.0147	0.0191	0.8
Cm_q	−34.2	0.6444	0.4314	1.5
$Cm_{\delta e}$	−1.74	0.0248	0.0131	1.9

[a] $s_E(\theta)$ = ensemble standard error.
[b] $s(\theta)$ = average program estimated standard error.

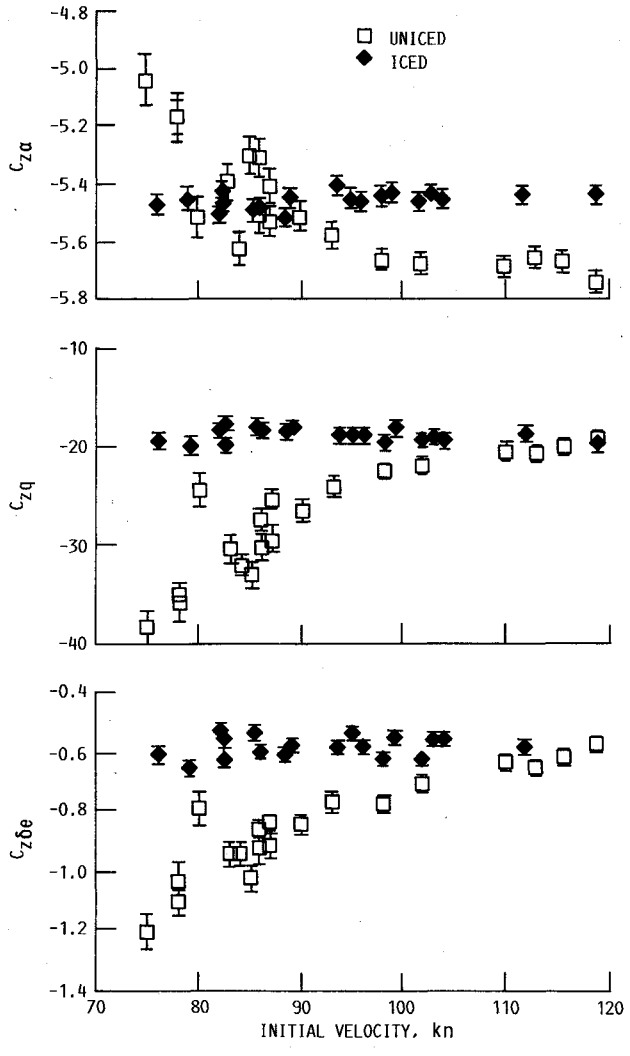

Fig. 4 Vertical force coefficient derivative estimates for 0-deg flap showing the effects of tail icing using the MSR technique; 2σ error bars are from the MSR program.

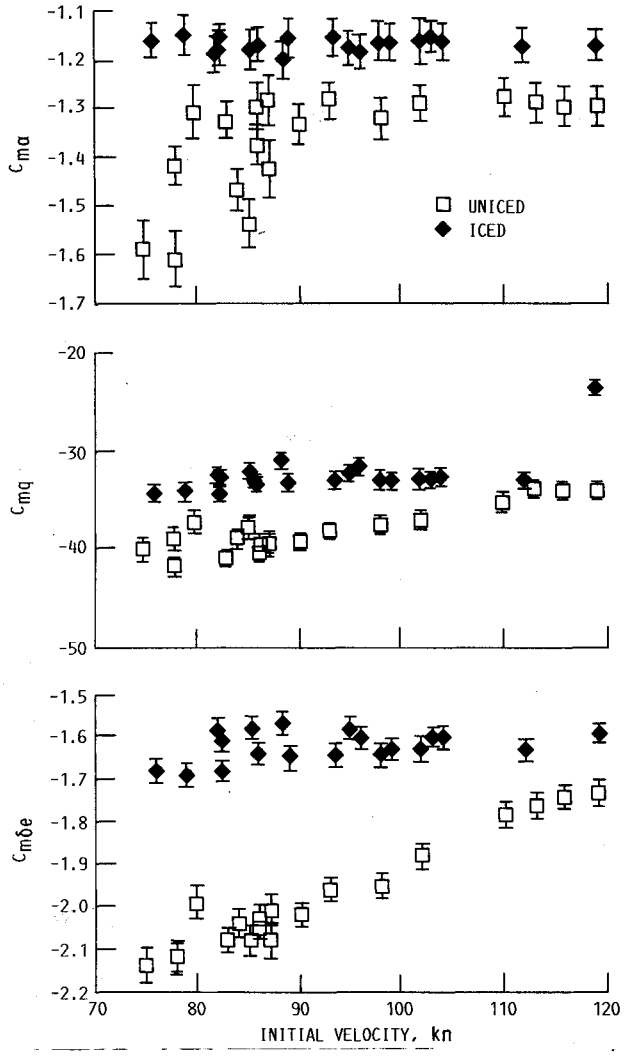

Fig. 5 Pitching moment coefficient derivative estimates for 0-deg flap showing the effects of tail icing using the MSR technique; 2σ error bars are from the MSR program.

and control variables from their initial steady-flight values, or combinations of those increments.

After postulating the aerodynamic model equations, the determination of significant terms among the candidate variables and estimation of the corresponding parameters follows. The variable chosen for entry into the regression equation is the one that has the largest correlation with y after adjusting for the effect on y of the variables already selected. The parameters are estimated by minimizing the cost function

$$J_{sr} = \sum_{i=1}^{N} \left[y(i) - \hat{\theta}_0 - \sum_{j=1}^{l} \hat{\theta}_j x_j(i) \right]^2 \qquad (2)$$

where N is the number of data points and $(l+1)$ is the number of parameters in the regression equation at any step.

At every step of the regression, the variables incorporated into the model in previous stages and a new variable entering the model are re-examined. Any variable that provides a nonsignificant contribution (due to correlation with more recently added terms) is removed from the model. The process of selecting and checking variables continues until no more variables are admitted to the equation and no more are rejected. Experience shows, however, that a model based on only the statistical significance of individual parameters in Eq. (1) can still include too many terms and, therefore, may have poor prediction capabilities. Several criteria for the selection of an adequate model are introduced in Ref. 7, and the details of the entire procedure are explained in that reference.

The analyses for the C_Z and C_m derivative estimates and the relative effects of tail icing on these estimates is given in Figs. 4–7. A physical interpretation of these results will be discussed in a later section of this report.

Accuracy of the Derivative Estimates

The 45 repeat doublet maneuvers, identically executed in each of the four configurations, provided a statistically significant data base for parameter and error estimate accuracy studies. The standard error calculated for each ensemble of parameter estimates verified the effectiveness of maneuver selection through demonstrated repeatability of the predicted parameters. In addition, a comparison of the average of the standard error values estimated by the computer program to the standard error for the ensemble provided an evaluation of how realistic the program estimated standard error values were.

Repeat maneuvers were analyzed using the MSR, and the resulting mean values of coefficients were compiled in Table 2. Accompanying each parameter estimate is the average standard error associated with it as given by the estimation algorithm, the standard error for the ensemble of values from the 45 repeat maneuvers, and the ratio of the two. The ratio given for each parameter is the factor by which the program estimated standard error for that parameter should be multiplied to produce a realistic expected standard error. For example, the standard error estimated by MSR for C_{Z_α} should

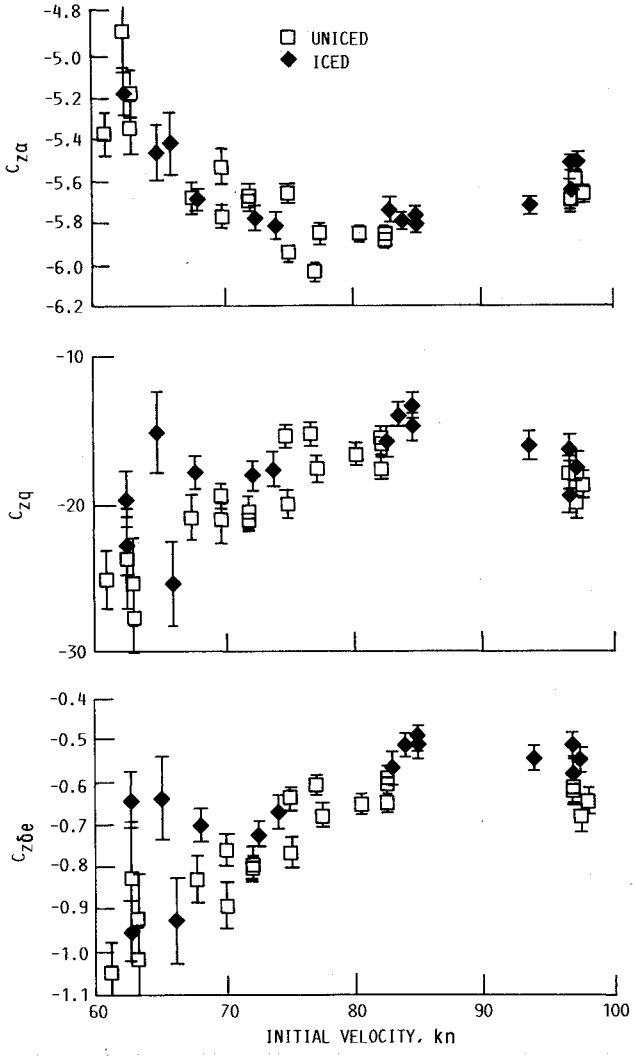

Fig. 6 Vertical force coefficient derivative estimates for 10-deg flap showing the effects of tail icing using the MSR technique; 2σ error bars are from the MSR program.

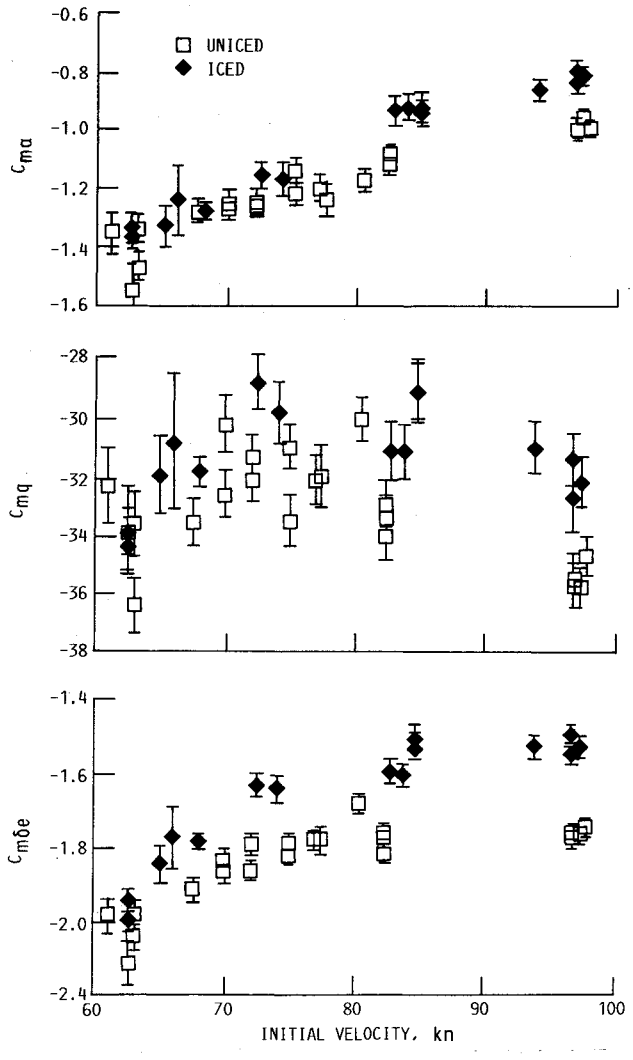

Fig. 7 Pitching moment coefficient derivative estimates for 10-deg flap showing the effects of tail icing using the MSR technique; 2σ error bars are from the MSR program.

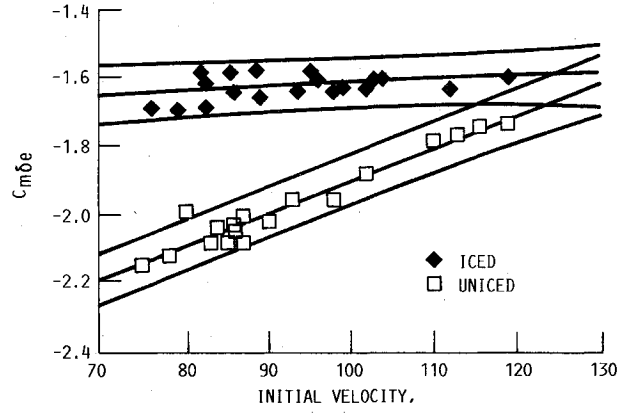

Fig. 8 Ninety-five percent confidence regions on elevator effectiveness values for the artificially iced vs uniced aircraft tail wing flaps at 0 deg.

be multiplied by 2.9 to achieve a realistic approximation to an actual ensemble standard error.

A fundamental issue throughout this research is that of distinguishing between the effects of ice and the inherent variability of predicted parameters. In addition to the error analysis performed on the values obtained from the 45 repeat maneuvers, the $C_{m_{\delta e}}$ estimates for the 0-deg flap condition were considered (Fig. 5c). This set of points was chosen for this portion of the analysis because each of the two groups of values (iced and uniced) lend themselves to linear approximations. Also, determining a 95% confidence region in this particular case serves to quantitatively enforce what is qualitatively a very noticeable difference in parameters for the iced/uniced cases. After approximating the two groups of points by straight lines, confidence regions about these lines were calculated according to Ref. 8.

The resulting region is one within which we can expect 95% of all predicted elevator effectiveness values to fall. Figure 8 presents these confidence regions and gives an illustration of both the areas in which icing effects are discernible as well as the speed range in which we cannot attribute any change in $C_{m_{\delta e}}$ to the artificial ice shape. A similar analysis can be done on other parameters by fitting them in a piecewise linear fashion.

Effects of Tail Ice on Handling Characteristics

The effects of icing on the horizontal tail plane were obtained by analyzing all of the doublet maneuvers executed throughout the attainable ranges of speed and angle of attack. The MSR analyzed results of these maneuvers, in the form of the estimated stability and control derivatives, are plotted with $\pm 2\sigma$ error bars based on the standard error as given by the computer program. The MSR analysis indicated that nonlinear terms were required for an adequate aerodynamic model.

Figures 4 and 5 show an analysis for the 0-deg flap cases. The C_Z derivatives indicate an apparent loss of elevator effectiveness, especially at low airspeeds that correspond with higher angles of attack. The pitching moment derivatives C_{m_α}, C_{m_q}, and $C_{m_{\delta e}}$, which have an important effect on airplane short-period stability and control characteristics, are also more strongly affected by the ice contaminated horizontal tail at low speeds. At higher speeds, the effects of tail ice become negligible. This analysis was supported by pilot comments reporting that, at low speeds, the "iced" airplane was less responsive to elevator control inputs and more weakly damped in pitch. These comments, however, were not based on specific piloting tasks normally used in assigning pilot ratings, but on the perceived relative differences (clean vs iced) in longitudinal control force, response, and pitching moment characteristics while performing parameter identification maneuvers.

In the 10-deg flap cases (Figs. 6 and 7), the effects of horizontal tail icing show an opposite trend when compared with the 0-deg cases. Analysis of the stability and control derivatives show slightly degraded pitching moment coefficients up to speeds of approximately 90 kt. Above these speeds, there is a more pronounced degradation in these derivatives, and this analysis was again verified by pilot comments. Doublet maneuvers performed at 100 kt with artificial tail ice were accompanied by elevator force lightening and a strong "burble" feedback in the controls at high negative pitch rates. This characteristic was assumed due to the high tail downwash angle induced in the pitch over portion of the doublet maneuver, causing a significant amount of separated flow to occur on the horizontal tail plane. This occurred at a low peak load factor of approximately 0 g.

Conclusions

Based on the analysis and results herein, two fundamental conclusions were drawn regarding the use of a modified stepwise regression algorithm in estimating the effects of icing on aircraft stability and control characteristics:

1) The effects of the artificial ice shape attached to the tail were measurable as changes in the longitudinal stability and control derivatives for all flight conditions tested and pilot comments regarding handling characteristics correlated with these findings.

2) A multiplicative relationship was identified between the ensemble standard error and the estimated standard error from the modified stepwise regression routine.

The numerical value representing the ratio of the ensemble standard error to the estimated standard error from the program when assigned to each control or stability derivative are indicative of the level of confidence one should have in the estimated value of that parameter.

The results of this first test program indicate that MSR is a viable technique for determining the effects of icing on the longitudinal stability and control characteristics of an aircraft. Application of this flight test and analysis technique should prove very useful for validating stability and control predictions from wind tunnels or computational methods.

Appendix: Postulated Models

The six degree-of-freedom equations of motion for the airplane are

$$\dot{u} = -qw + rv - g\sin\theta + \frac{\rho V^2 S}{2m} C_X \tag{A1}$$

$$\dot{v} = -ru + pw + g\cos\theta\sin\phi + \frac{\rho V^2 S}{2m} C_Y \tag{A2}$$

$$\dot{w} = -pv + qu + g\cos\theta\cos\phi + \frac{\rho V^2 S}{2m} C_Z \tag{A3}$$

$$\dot{p} = qr\left[\frac{I_Y - I_Z}{I_X}\right] + \frac{I_{XZ}}{I_X}(pq + \dot{r}) + \frac{\rho V^2 Sb}{2I_X} C_l \tag{A4}$$

$$\dot{q} = pr\left[\frac{I_Z - I_X}{I_Y}\right] + \frac{I_{XZ}}{I_Y}(r^2 - p^2) + \frac{\rho V^2 S\bar{c}}{2I_Y} C_m \tag{A5}$$

$$\dot{r} = pq\left[\frac{I_X - I_Y}{I_Z}\right] + \frac{I_{XZ}}{I_Z}(\dot{p} - qr) + \frac{\rho V^2 Sb}{2I_Z} C_n \tag{A6}$$

along with kinematic relations

$$\dot{\theta} = q\cos\phi - r\sin\phi \tag{A7}$$

$$\dot{\phi} = p + (q\sin\phi + r\cos\phi)\tan\theta \tag{A8}$$

where a dot over a symbol represents the derivative with respect to time. The total airspeed V is given by

$$V = (u^2 + v^2 + w^2)^{1/2}$$

Here, Eqs. (A1), (A3), (A5), and (A7) describe the longitudinal motion, whereas Eqs. (A2), (A4), (A6), and (A8) describe the lateral motion of the airplane. The angles of attack and side slip are given by

$$\alpha = \tan^{-1}(w/u)$$

$$\beta = \sin^{-1}(v/V)$$

The aerodynamic forces and moments are represented by the coefficients $C_a(a = X, Y, Z, l, m, \text{or } n)$. It is postulated that these coefficients can be written as a Taylor's series polynomial expansion about an equilibrium trim condition as

$$C_a = \Theta_{a,0} + \sum_{j=1}^{l} \Theta_{a,j}\, \Delta x_j \qquad \text{(A9)}$$

where $\Theta_{a,0}$ and $\Theta_{a,j}$ are the unknown parameters. For $a = X$, Z, or m, the independent variables x_j are α, $(q\bar{c})/(2V)$, δe, and their combinations. For $a = Y$, l, or n, they are β, $(pb)/(2V)$, $(rb)/(2V)$, δ_a, δ_r, and their combinations. Furthermore,

$$\Delta x_j = x_j(t) - x_j(t = 0)$$

References

[1]Ranaudo, R. J., Mikkelsen, K. L., McKnight, R. C., and Perkins, P. J., Jr., "Performance Degradation of a Typical Twin Engine Computer Type Aircraft in Measured Natural Icing Conditions," AIAA Paper 84-0179, Jan. 1984.

[2]Mikkelsen, K. L., McKnight, R. C., Ranaudo, R. J., and Perkins, P. J., Jr., "Icing Flight Research: Aerodynamic Effects of Ice and Ice Shape Documentation with Stereo Photography," AIAA Paper 85-0468, Jan. 1985.

[3]Ranaudo, R. J., et al., "The Measurement of Aircraft Performance and Stability and Control After Flight Through Natural Icing Conditions," AIAA Paper 86-9758, April 1986.

[4]Jordan, J. L., Platz, S. J., and Schinstock, W. C., "Flight Test Report of the NASA Icing Research Airplane," Kohlman Systems Research, Inc., Lawrence, KS, KSR 86-01, Oct. 1986.

[5]Maine, R. E., and Iliff, K. W., "Application of Parameter Estimation to Aircraft Stability and Control: The Output-Error Approach," NASA RP-1168, June 1986.

[6]Klein, V., and Morgan, D. R., "Estimation of Bias Errors in Measured Airplane Responses Using Maximum Likelihood Method," NASA TM-89059, Jan. 1987.

[7]Klein, V., Batterson, J. G., and Murphy, P. C., "Determination of Airplane Model Structure from Flight Data By Using Modified Stepwise Regression," NASA TP-1916, Oct. 1981.

[8]Daniel, C., and Wood, F. S., *Fitting Equations to Data*, Wiley, New York, 1980.